

Periodically focused modes in chains of dielectric spheres

Arash Darafsheh and Vasily N. Astratov

Citation: *Appl. Phys. Lett.* **100**, 061123 (2012); doi: 10.1063/1.3684246

View online: <http://dx.doi.org/10.1063/1.3684246>

View Table of Contents: <http://apl.aip.org/resource/1/APPLAB/v100/i6>

Published by the [American Institute of Physics](#).

Related Articles

Bloch surface waves-controlled fluorescence emission: Coupling into nanometer-sized polymeric waveguides
Appl. Phys. Lett. **100**, 063305 (2012)

Enhanced spontaneous emission from quantum dots in short photonic crystal waveguides
Appl. Phys. Lett. **100**, 061122 (2012)

Transmission enhancement in a non-adiabatic tapered nano-aperture waveguide
Appl. Phys. Lett. **100**, 051104 (2012)

Vertical waveguides integrated with silicon photodetectors: Towards high efficiency and low cross-talk image sensors
Appl. Phys. Lett. **100**, 043504 (2012)

Optical planar waveguide for cell counting
Appl. Phys. Lett. **100**, 043701 (2012)

Additional information on *Appl. Phys. Lett.*

Journal Homepage: <http://apl.aip.org/>

Journal Information: http://apl.aip.org/about/about_the_journal

Top downloads: http://apl.aip.org/features/most_downloaded

Information for Authors: <http://apl.aip.org/authors>

ADVERTISEMENT



LakeShore Model 8404 developed with **TOYO Corporation**
NEW AC/DC Hall Effect System Measure mobilities down to 0.001 cm²/V s

Periodically focused modes in chains of dielectric spheres

Arash Darafsheh and Vasily N. Astratov^{a)}

Department of Physics and Optical Science, Center for Optoelectronics and Optical Communications, University of North Carolina at Charlotte, Charlotte, North Carolina 28223-0001, USA

(Received 25 December 2011; accepted 24 January 2012; published online 10 February 2012)

We show that, theoretically, Brewster angle conditions for transverse magnetic polarized rays can be periodically reproduced in chains of spheres with index $n = \sqrt{3}$ giving rise to lossless periodically focused modes with $2D$ period, where D is the sphere diameter. Using ray tracing for a spherical emitter with the diameter D we show that chains of spheres work as filters of such modes at $1.72 < n < 1.85$. This leads to tapering of the focused beams combined with the reduction of their attenuation along the chain. Experimentally, the “beam tapering” effect was observed in chains of $300\ \mu\text{m}$ sapphire spheres with index ~ 1.77 in visible. © 2012 American Institute of Physics. [doi:10.1063/1.3684246]

It is well accepted that a set of identical lenses can be used to relay light between two locations.¹ The optical losses of such periodically focusing waveguides (PFWs) have been considered to be high since the lenses are usually partially reflective. For example, by integrating TE and TM components of the linearly polarized incident plane wave over a sphere with index $n = 1.58$ immersed in water, one can estimate total reflection losses about 0.27 dB/sphere.² Recently, however, fabrication of extremely long and well ordered chains of microspheres has become possible by self-assembly techniques that stimulated a great deal of interest in their optical properties.^{3–11} Initially, this interest was focused on coupling between whispering gallery modes (WGMs) in spheres.^{4,5} The notable advance in this area has been the identification of two distinct mechanisms of optical transport: (i) evanescent WGM coupling and (ii) nanojet coupling based on periodic focusing.⁶ The terminology of photonic nanojets came from tightly focused beams produced by single microspheres.^{12–14} It was shown that the properties of chains are determined by nanojet-induced modes (NIMs) with the period equal to the size of two spheres ($2D$).^{7,8} Both mechanisms have been observed in chains of polystyrene microspheres with D in $2\text{--}10\ \mu\text{m}$ range.^{7–11}

These studies have revealed two effects which still remain poorly understood at the present time. Both effects were observed when such chains were optically coupled to multimodal sources of light such as dye-doped fluorescent microspheres. The first is an extraordinarily small attenuation of light ~ 0.08 dB/sphere observed in such chains at long distances from the light source.⁸ The second effect is connected with a gradual decrease of the lateral width of the beams that are focused periodically along the chains.⁷ The latter effect has already found application for focusing multimodal mid-infrared beams in laser-tissue surgery.^{15,16}

In this work we study PFWs in the limit of geometrical optics which is a reasonable approximation for $D \gg 10\ \lambda$, where λ is the wavelength of light. We show that in principle, when $n = \sqrt{3}$ a special type of TM polarized incident ray

propagates through the chain *without attenuation* under Brewster angle conditions. These rays give rise to periodic focused modes (PFMs) with the period $2D$ and radial polarization, which can be considered as a geometrical optics analog of NIMs observed in earlier work using micron-scale polystyrene microspheres.^{7–11} From numerical ray tracing we show that chains of spheres are natural PFM filters that lead to beam tapering effects and dramatic reductions of attenuation for $1.72 < n < 1.85$. We observed such beam tapering in chains of sapphire ($n \sim 1.77$) microspheres with $D = 300\ \mu\text{m}$ and showed very good agreement between the results and the theory.

In our modeling we used a spherical light source (S) in contact with the same size spheres, as shown in Fig. 1(a). We assumed a uniform distribution of the point sources of rays with random polarizations and directions inside the source S. Such source has two advantages. First, it allows a direct comparison of the results with experiments performed using fluorescent dye-doped spheres. Second, all spatial

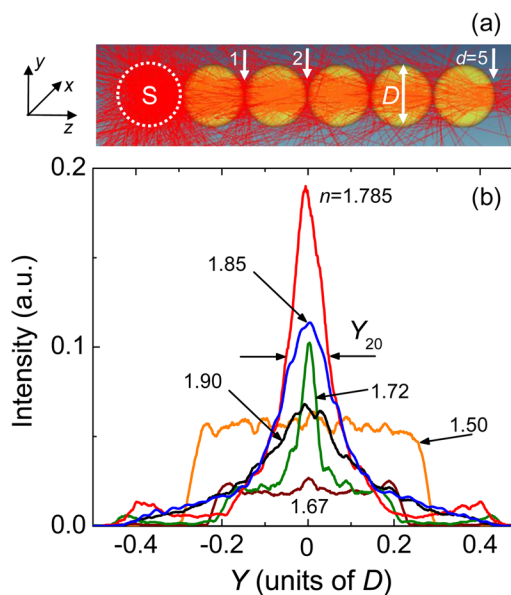


FIG. 1. (Color online) (a) Ray tracing for five-sphere chain with $n = 1.785$. (b) Intensity profiles calculated for twenty-sphere chains with different n . FWHM is indicated as $Y_{20} \sim 0.1$ for a profile corresponding to $n = 1.785$.

^{a)}Electronic mail: astratov@uncc.edu.

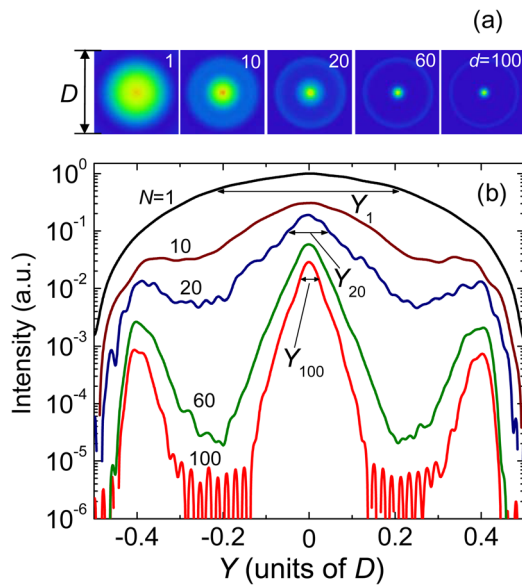


FIG. 2. (Color online) (a) Intensity patterns and (b) profiles calculated at different distances from the source S for $n = 1.785$.

dependencies scale with D , which permits use of dimensionless units: $X = x/D$, $Y = y/D$, and $Z = z/D$. We used the ray tracing software ZEMAX-EE (Radiant Zemax, Bellevue, WA) which takes into account the Fresnel reflections and refractions at the spherical interfaces. This leads both to a gradual attenuation of initial rays once they propagate through the structure and to the emergence of new rays. We traced the rays down to a weight factor (WF) of 10^{-3} which provided good convergence of the numerical solutions. The XY beam profiling was performed at the positions where the spheres touch using a flat detector with unit size and square shape. It

was placed at different distances ($d = 1, 2, \dots, N$) measured in dimensionless units from the right vertex of the S-sphere, as shown in Fig. 1(a). The intensity distributions were calculated from the density of the rays at the detector plane with their WF taken into account.

The beam reshaping that occurs as a function of n is illustrated in Fig. 1(b) for a 20-sphere long chain. It is seen that for $n = 1.5$ and 1.67 the beam has almost uniform radial intensity distribution with the full width at half maximum (FWHM) $Y_{20} \sim 0.4-0.5$. However, for $n = 1.72, 1.785$, and 1.85 the central section of the beam acquires a quasi-Gaussian shape with much narrower FWHM. For $n = 1.785$, this is indicated by $Y_{20} \sim 0.1$. Further increase of n leads to beam broadening, as illustrated for $n = 1.90$.

The evolution of the beam profile at different distances (d) from the S-sphere for a chain with $n = 1.785$ is represented in Figs. 2(a) and 2(b). After the first sphere ($d = 1$) the beam has a quasi-Gaussian shape with FWHM $Y_1 \sim 0.45$ as shown in Fig. 2(b). After propagation through ten spheres, the beam profile displays a narrower central peak superimposed on a wide and flat background. After 100 spheres, the central peak becomes extraordinary narrow and $Y_{100} \sim 0.04$. In addition, an extremely narrow “ring” with diameter ~ 0.8 and much weaker peak intensity than the central peak is formed. The gradual tapering of the central beam accompanied by a ring formation is readily seen in the calculated intensity patterns in Figs. 2(a) and 2(b).

We propose an interpretation of these observed effects based on introducing a PFM mechanism. As schematically illustrated in Fig. 3(a) there is a special type of TM polarized rays, incident parallel to the axis of the system, which propagate in such chains without losses in the limit of geometrical optics. This occurs when external θ and consequently

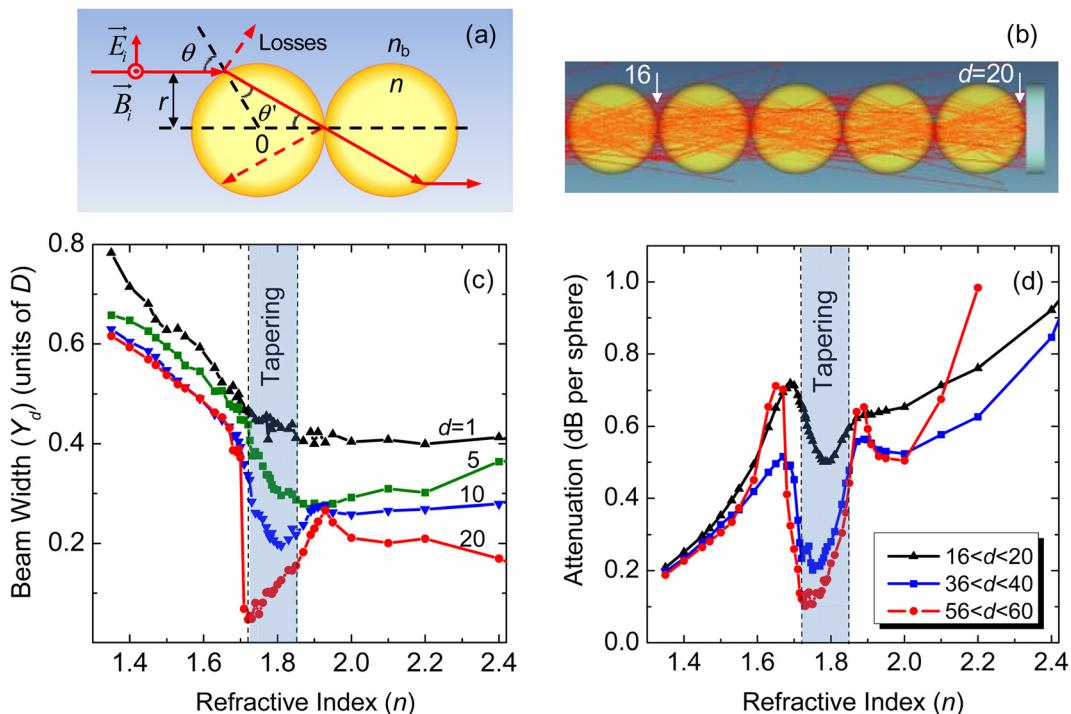


FIG. 3. (Color online) (a) TM polarized meridional ray with the directions of incident electric (\vec{E}_i) and magnetic (\vec{B}_i) vectors indicated, (b) ray tracing from 16th to 20th sphere for $n = 1.785$, (c) FWHM of the central peak calculated as a function of n at different distances (d) from the source, (d) attenuation per sphere as a function of n calculated for different segments of the chain.

internal θ' angles of incidence are equal to the corresponding Brewster's angles. These conditions are periodically reproduced (with a period of $2D$) when the refracted ray passes through the point where the spheres touch leading to the following equation:

$$\tan^{-1}(n/n_b) = 2\tan^{-1}(n_b/n), \quad (1)$$

where n_b is the index of the background medium. In this work it is assumed that $n_b = 1$. This equation has a solution at $n/n_b = \sqrt{3}$, $\theta = \pi/3$, and $r = \sqrt{3}/4$ in dimensionless units. In physical optics, such rays correspond to PFMs with axial symmetry, radial polarization, $2D$ period along z , and extremely small losses. Similar to the modes in fibers, PFMs should have properties determined by the phase; however, these properties are beyond the scope of this work.

In geometrical optics, the key property is the fact that although the illumination provided by the S-sphere contains a variety of meridional and skew rays, only PFMs survive in the long chains. Our ray tracing shows that these PFM filtering properties are actually preserved in a range of indices from 1.72 to 1.85. This is illustrated for $n = 1.785$ in Fig. 3(b), which shows two fundamental PFMs shifted by D in a $16 < d < 20$ section of the chain. The beam tapering effect can be explained by these filtering properties since PFMs are

sharply focused. The “ring” pattern appears due to filtering the second PFM shifted by D .

This interpretation is consistent with the results of modeling for a broad range of parameters n and d presented in Figs. 3(c) and 3(d). The tapering of the central beam is clearly seen over the $1.72 < n < 1.85$ range at $d \geq 10$ in Fig. 3(c). The reduction of the attenuation of the total transmitted power over this range of indices is evident in Fig. 3(d) with the local minimum of attenuation ~ 0.1 dB/sphere attained at $n = 1.72$ - 1.75 for a $56 < d < 60$ section of the chain.

Experimentally, the light focusing properties were studied and compared in chains of sapphire (Swiss Jewel Company, $n \sim 1.77$, $D = 300 \pm 3 \mu\text{m}$) and polystyrene (Thermo Fisher Sci., $n \sim 1.59$, $D = 289 \pm 6 \mu\text{m}$) microspheres. The chains were assembled on glass substrates using a micro needle controlled by a hydraulic micromanipulator, as illustrated in Fig. 4(a). The source used was a single dye-doped fluorescent (FL) polyethylene sphere (Cospheric, Santa Barbara, CA) with $D \sim 300 \mu\text{m}$. The FL excitation was provided at 340-370 nm by a mercury lamp integrated with an inverted IX-71 Olympus microscope. The FL emission occurred in a 490-570 nm band having a maximum at 530 nm. A small fraction of the total emitted power was coupled to the chain. The propagation effects were made visible as a result of light scattering away from the axis of the chain, as shown in Fig. 4(a).

An image of the bright region at the “shadow” surface of a single sphere attached to the S-sphere was obtained with focusing at its equatorial plane. This is illustrated in Fig. 4(b). We assumed that due to surface scattering the brightness along the equator of the sphere is representative of the local intensity of the beam guided by the chain in the axial direction. This allows a simple estimation of the beam FWHM using the envelope of the maxima of the intensity profiles measured along closely spaced lines A-F, as illustrated in Fig. 4(c). Similar measurements performed for chains of sapphire ($n \sim 1.77$) and polystyrene (~ 1.59) spheres with variable length show the pronounced beam tapering effect in the former case very well and the absence of this effect in the latter case, as illustrated in Fig. 4(d). Very good agreement of the normalized beam FWHMs (Y_d/Y_1) with modeling was found in both cases.

In this work we introduced the PFM concept in geometrical optics based on neglecting the interference and diffraction effects in such structures. Thus, the results are applicable to sufficiently large spheres ($D/\lambda \gg 10$). In addition, the focused beams should have sufficiently large FWHMs that are well in excess of diffraction limited dimensions, i.e., $Y_d > \lambda/D$. Using a spherical light source, we showed that chains of spheres work as PFM filters when $1.72 < n < 1.85$. This phenomenon leads to gradual tapering of the beams, combined with a reduction in their attenuation along the chain. Previously we performed numerical ray tracing for three- and five-sphere chains assembled inside hollow waveguides where we observed focused beams with progressively smaller lateral dimensions at $1.65 < n < 1.75$.¹⁶ The fact that in the present work the beam tapering effect takes place at higher indices $1.72 < n < 1.85$ is connected with much broader directionality of the spherical light source. The results of the present work scale with D and can be used

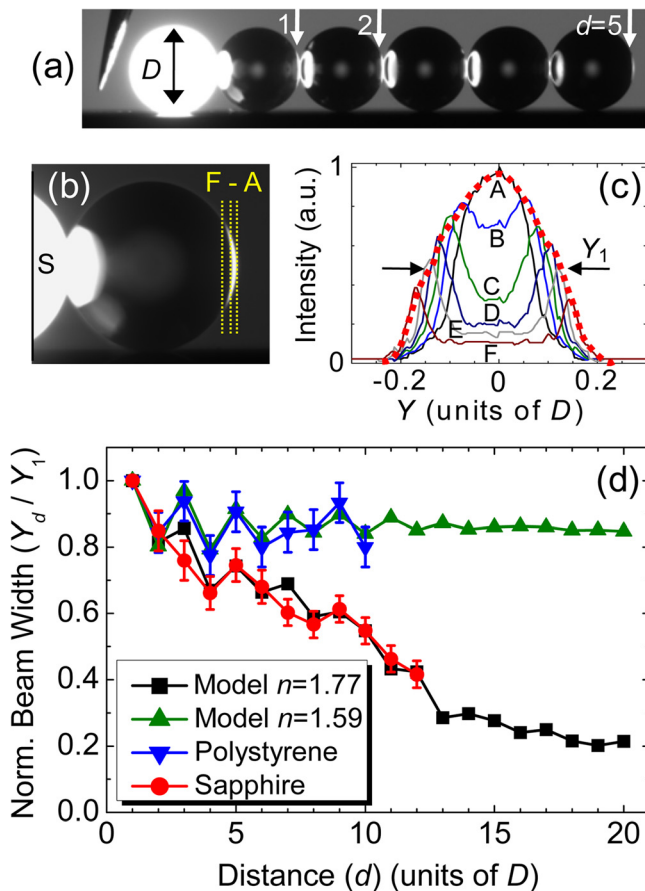


FIG. 4. (Color online) (a) A chain of $300 \mu\text{m}$ sapphire microspheres in contact with a dye-doped S-sphere, (b) expanded image of the scattered light at the “shadow” surface of the sapphire sphere, (c) envelope (dashed) of the maxima of the A-F intensity profiles with its FWHM shown as Y_1 , (d) normalized beam FWHM (Y_d/Y_1) measured for sapphire and polystyrene sphere chains and comparison with the modeling for $n = 1.77$ and 1.59 , respectively.

for developing light focusing devices coupled with multimodal light sources.^{15,16} Examples of such applications include ultra-precise laser procedures in the eye¹⁶ and brain or piercing a cell, as well as for coupling light into photonic microstructures. A particularly interesting direction of future studies is connected with the polarization properties of PFMs resembling that for radially polarized light beams which have been used for achieving sharper focal spots.¹⁷ Another interesting possibility is based on using microspheres made from optically nonlinear and/or active materials where a combination of sharp focusing with periodicity should result in efficient optical parametric and lasing processes.

The authors thank A. Lupu, M. Tchernycheva, N. M. Fried, and M. A. Fiddy for stimulating discussions. The authors gratefully acknowledge support for our work from the National Eye Institute under Award Number R41EY019598. The content is solely the responsibility of the authors and does not necessarily represent the official views of the National Eye Institute or the National Institutes of Health. This work was also supported by the U.S. Army Research Office through Dr. J. T. Prater under Contract No. W911NF-09-1-0450 and by the National Science Foundation under grant ECCS-0824067.

¹B. E. A. Saleh and M. C. Teich, *Fundamentals of Photonics*, 2nd ed. (John Wiley & Sons, Hoboken, New Jersey, 2007).

²A. Ashkin, *Phys. Rev. Lett.* **24**, 156 (1970).

³V. N. Astratov, *Photonic Microresonator Research and Applications*, Springer Series in Optical Sciences Vol. 156, edited by I. Chremmos, O. Schwelb, and N. Uzunoglu (Springer, New York, 2010), pp. 423–457.

⁴V. N. Astratov, J. P. Franchak, and S. P. Ashili, *Appl. Phys. Lett.* **85**, 5508 (2004); A. V. Kanaev, V. N. Astratov, and W. Cai, *ibid.* **88**, 111111 (2006); S. P. Ashili, V. N. Astratov, and E. C. H. Sykes, *Opt. Express* **14**,

9460 (2006); V. N. Astratov and S. P. Ashili, *ibid.* **15**, 17351 (2007); S. Yang and V. N. Astratov, *Opt. Lett.* **13**, 2057 (2009).

⁵T. Mukaiyama, K. Takeda, H. Miyazaki, Y. Jimba, and M. Kuwata-Gonokami, *Phys. Rev. Lett.* **82**, 4623 (1999); Y. P. Rakovich, J. F. Donegan, M. Gerlach, A. L. Bradley, T. M. Connolly, J. J. Boland, N. Gaponik, and A. Rogach, *Phys. Rev. A* **70**, 051801 (2004); B. M. Möller, U. Woggon, M. V. Artemyev, and R. Wannemacher, *Phys. Rev. B* **70**, 115323 (2004); Y. Hara, T. Mukaiyama, K. Takeda, and M. Kuwata Gonokami, *Phys. Rev. Lett.* **94**, 203905 (2005); C. S. Deng, H. Xu, and L. Deych, *Opt. Express* **19**, 6923 (2011).

⁶Z. Chen, A. Taflove, and V. Backman, *Opt. Lett.* **31**, 389 (2006).

⁷A. M. Kapitonov and V. N. Astratov, *Opt. Lett.* **32**, 409 (2007).

⁸S. Yang and V. N. Astratov, *Appl. Phys. Lett.* **93**, 261111 (2008).

⁹M. Gerlach, Y. P. Rakovich, and J. F. Donegan, *Opt. Express* **15**, 17343 (2007).

¹⁰T. Mitsui, Y. Wakayama, T. Onodera, Y. Takaya, and H. Oikawa, *Opt. Lett.* **33**, 1189 (2008); T. Mitsui, Y. Wakayama, T. Onodera, T. Hayashi, N. Ikeda, Y. Sugimoto, T. Takamasu, and H. Oikawa, *Adv. Mater.* **22**, 3022 (2010); T. Mitsui, T. Onodera, Y. Wakayama, T. Hayashi, N. Ikeda, Y. Sugimoto, T. Takamasu, and H. Oikawa, *Opt. Express* **19**, 22258 (2011).

¹¹O. Lecarme, T. P. Rivera, L. Arbez, T. Honegger, K. Berton, and D. Peyrade, *J. Vac. Sci. Technol. B* **28**, C6011 (2010).

¹²Z. Chen, A. Taflove, and V. Backman, *Opt. Express* **12**, 1214 (2004); A. Heifetz, S. C. Kong, A. V. Sahakian, A. Taflove, and V. Backman, *J. Comput. Theory Nanosci.* **6**, 1979 (2009); S. Yang, A. Taflove, and V. Backman, *Opt. Express* **19**, 7084 (2011).

¹³P. Ferrand, J. Wenger, A. Devilez, M. Pianta, B. Stout, N. Bonod, E. Popov, and H. Rigneault, *Opt. Express* **16**, 6930 (2008); A. Devilez, N. Bonod, J. Wenger, D. Gérard, B. Stout, H. Rigneault, and E. Popov, *ibid.* **17**, 2089 (2009).

¹⁴Yu. E. Geints, A. A. Zemlyanov, and E. K. Panina, *J. Opt. Soc. Am. B* **28**, 1825 (2011); Photonic Jets from Resonantly-Excited Transparent Dielectric Microspheres *ibid.* (to be published).

¹⁵V. N. Astratov, International patent publication WO/2011/005397 (17 June 2009).

¹⁶A. Darafsheh, A. Fardad, N. M. Fried, A. N. Antoszyk, H. S. Ying, and V. N. Astratov, *Opt. Express* **19**, 3440 (2011).

¹⁷S. Quabis, R. Dorn, M. Eberler, O. Glockl, and G. Leuchs, *Opt. Commun.* **179**, 1 (2000); R. Dorn, S. Quabis, and G. Leuchs, *Phys. Rev. Lett.* **91**, 233901 (2003).